ePDH online.com

Credit: 2 PDH

Course Title:

Spray Pyrolysis Processing for Optoelectronic Applications

Approved for Credit in All 50 States

Visit epdhonline.com for state specific information including Ohio's required timing feature.

3 Easy Steps to Complete the Course:

1. Read the Course PDF
2. Purchase the Course Online & Take the Final Exam
3. Print Your Certificate

Chapter 8

Spray Pyrolysis Processing for Optoelectronic Applications

Oleksandr Malik,
Francisco Javier De La Hidalga-Wade and
Raquel Ramírez Amador

Additional information is available at the end of the chapter

http://dx.doi.org/10.5772/67431

Abstract

Spray pyrolysis is a low-cost and simple technique for the fabrication of high-quality transparent and conducting oxide thin films for different optoelectronic applications. The fabrication method, structural, morphological, and electro-optical properties of fluorine-doped tin oxide (FTO) and tin-doped indium oxide (ITO) films have been investigated. The deposited films have low resistivity and high transparency. Applications of such films are shown in high-efficiency surface-barrier photodetectors and solar cells, where the films serve as an active and antireflection electrode. A short description of other undoped and doped oxide films such as ZnO and TiO_2 fabricated by spray pyrolysis is presented.

Keywords: spray pyrolysis, thin film, fluorine-doped tin oxide, tin-doped indium oxide, surface-barrier photodetectors, solar cells

1. Introduction

It is well known that some thin oxide films that are heavily doped n-type semiconductors present both high conductivity and high transparency. Materials exhibiting simultaneously both high conductivity and optical transmittance are named transparent conducting oxides (TCOs). The most representative of such materials are tin-doped indium oxide (In_2O_3) and fluorine-doped tin oxide (SnO_2), known as ITO and FTO, respectively. These materials have been thoroughly studied due to their innumerable optoelectronic applications for devices, such as in solar cells, liquid crystal displays, organic light-emitting diodes, and heat mirrors [1]. A number of techniques, such as oxidation of metal films, sputtering, chemical vapor deposition, and

growth from chemical solutions, have been investigated in the search for the most reliable and cheapest fabrication method of the TCO thin films [1]. Chemical fabrication techniques have been studied extensively due to their simplicity, low-cost, and the flexibility for the doping process. The spray pyrolysis processing is one of the most simple fabrication method that has been known for more than three decades since the first published work in 1966 when it was used for the spray-deposited CdS films [2]. Because of the simplicity of the technical apparatus used as well as the inherent suitability for large-scale production, the spray pyrolysis is the most attractive method for the TCO films fabrication. This method presents a numbers of advantages [3] such as the extremely easy way of doping the films by adding certain elements to the spray solution, the process is conducted in air ambient (vacuum conditions are not required) and operated at moderate temperatures, resulting into a compact and simple fabrication process. The aim of this chapter is to describe the fabrication method and properties of some useful TCO films and their optoelectronic properties suitable for applications as transparent ohmic contacts in thin film solar cells as well as an active and antireflection electrode in the design of efficient surface-barrier semiconductor photodetectors. Recently, the quite important optoelectronic application of this method for the fabrication of efficient silicon solar cells and modules has been reported [4]. Readers can find many such applications of the TCO films in the literature.

2. Spray pyrolysis processing: general remarks

Spray pyrolysis is a process in which a thin film is deposited by spraying a solution on a heated surface, where the constituents react to form a chemical compound [5]. The chemical spray deposition process, according to the type of reaction, can be divided into three groups [6]: In the first group, the droplets of the solution reside on the heated surface as the solvent evaporates and components may further react in the dry state. The second group represents a process in which the solvent evaporates before the drops reach the heated surface and the dry solid impinges on the surface by decomposition. In the third group, there are processes where the solvent vaporizes as the droplets approach the substrate with the consequent heterogeneous reaction of the solution components. The most important parameters to be controlled in all of these processes are the substrate temperature, carrier gas flow rate, nozzle-to-substrate distance, and the solution content and concentration. Among these variables, the substrate temperature has been considered as the most important factor in producing thin film from spray pyrolysis processing; this is because the droplets drying, decomposition, crystallization, and grain growth depend strongly on this parameter [7]. The main part of the apparatus used for the spray pyrolysis deposition is the atomizer for obtaining aerosol from the precursor solution. The design of this equipment can be variable from inexpensive cosmetics or perfume purpose atomizers [8, 9] through a Pyrex glass or metallic individual or commercial design atomizers to much more complicated ultrasonic equipments [10]. Despite the apparent simplicity of the spray pyrolysis technique, a tight correlation of the deposition parameters called for a theoretical modeling spray pyrolysis deposition [11], the aim of which was the understanding of this correlation with the optimization of the deposition process. Such modeling examines the changing of the films topography, where the droplets can be seen as

http://dx.doi.org/10.5772/67431

a flux and not as individual drops, and when they evaporate near the surface prior to fully contacting the substrate in liquid form. A typical spray deposition system includes the spray atomizer containing the precursor solution, a heater for the substrate, pressurized air, liquid flow, and temperature controllers. Inherently, to the spray process, the thickness of the film can be nonuniform, thus a random motion of the spray nozzle or the substrate is useful for an uniform deposition [5]. The following sections of this chapter are dedicated to the description of the experimental method for the deposition of thin TCO films, as well to show their structural, electric, and optical properties for their applications in designing different optoelectronic devices. Our research activity in this field started by 1979 [12, 13] when the spray pyrolysis was used for the fabrication of silicon solar cells.

3. Spray-deposited fluorine-doped tin oxide films

Figure 1 shows schematical representation of our spraying system [4]. It produces films presenting uniform thicknesses for spraying areas of few square centimeters by a mechanical moving of a Pyrex glass spray head.

The substrate holder is a graphite block mounted on the electric heater, the temperature of which is controlled by a thermocouple. To prevent a rapid cooling of the substrate by

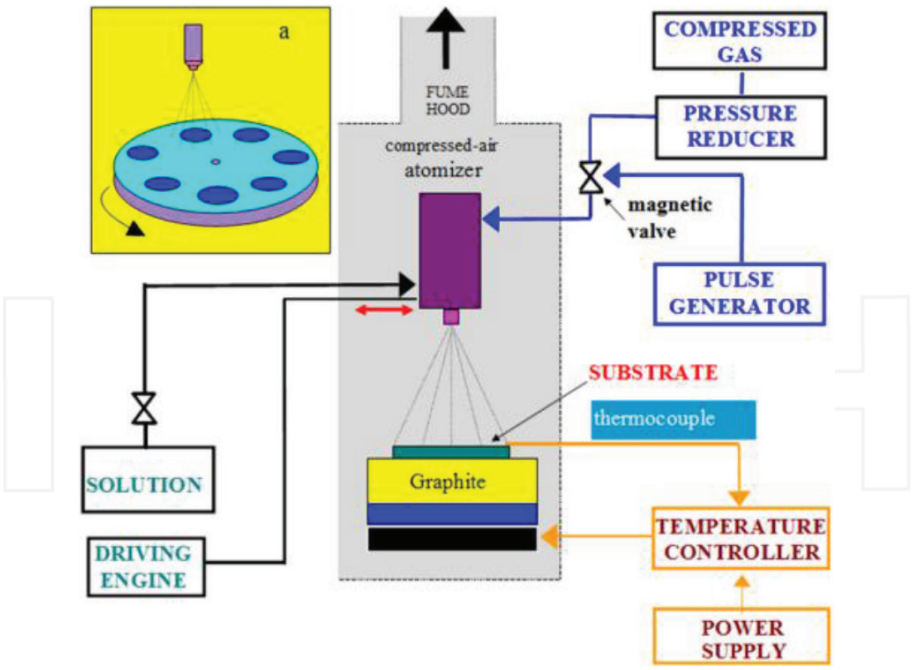

Figure 1. Schematical representation of our spraying system.

the spraying solution, the compressed air is injected into the atomizer during a short time (around 1–2 s) with a long pause (10–30 s); this period of time is controlled by the magnetic valve. Thus, the pulsed spraying leads to the deposition of uniform films. The fixed temperature (480°C) is controlled and supported by a microprocessor. The inset of **Figure 1** shows the holder modification for deposition of TCO films on semiconductor wafers with large areas. The film thickness depends on several parameters: the distance between the spray nozzle and the substrate, the substrate temperature, the concentration of the precursor solution, and the deposition time.

The deposition method used in this work was conducted, using compressed air at a pressure of 0.5 atm and a Pyrex atomizer located at 30 cm from either the Corning glass or the sapphire substrate [14]. Additional technological parameters are shown in **Table 1**. A 0.2 M solution of tin (IV) chloride pentahydrate ($SnCl_4 \cdot 5H_2O$) dissolved in methanol was used as the starting solution. A small amount of ammonium fluoride (NH_4F) dissolved in water was added in the starting solution for the preparation of the precursor with a 0–1 F/Sn molar ratio (**Table 2**). Since the presence of water can lead to the hydrolysis of the tin chloride, we added a few drops of hydrochloric acid (HCl) into the precursor solution; a 10 ml/min precursor flow rate was used for this deposition process [14].

The films' thickness was measured using an Alpha Step 200 profilometer. The X-ray diffraction (XRD) measurements were carried out with an X-ray diffractometer Brucker AXS D8 Advance, with a Cu cathode (1.54059 Å) operating in the Bragg-Brentano Two-Theta geometry. An atomic force microscope JEOL JSPM-4310 was used to study the films' surface. The electrical resistivity (ρ) and carrier density (n_e) were measured at room temperature using the standard van der Pauw method, where the Hall effect parameters were obtained for a magnetic field of 0.3 T. Finally, the optical properties were measured using the Agilent-8453 (200 nm a 1100 nm) spectrophotometer.

The XRD measurements of the FTO films with different F/Sn ratios in the solution are shown in **Figure 2**.

Transporting gas	**Compressed air**
Pressure of the gas	3 kg/cm^2
Diameter of nozzle	2 mm
Distance nozzle-substrate	30 cm
Temperature of the substrate	450 ± 5°C
Tin concentration in solution	0.2 M
Atomic ratio of F/Sn in the solution	0.0–1.0
Time of a single deposition step	1 s
Time of a single cooling period	2 s

Table 1. Technological parameters used for the deposition of the FTO films.

F/Sn molar ratio	NH_4F, mg	$SnCl_4 \cdot 5H_2O$, g	$H_2O + CH_3CH_2OH$ (1:3), ml
0	0	1.519	15
0.20	22.22	1.519	15
0.35	38.89	1.519	15
0.50	55.56	1.519	15
0.65	72.23	1.519	15
0.85	94.45	1.519	15
1	111.12	1.519	15

Table 2. Content of the precursor solutions for fabrication of fluorine-doped tin oxide (FTO) films with different F/Sn ratios.

Figure 2 presents the X-ray diffraction (XRD) measurements for the FTO deposited; it can be seen, according to the American Society for Testing and Materials standard for tin oxides [15], that the films with a thickness around 500 nm have a tetragonal rutile structure since they show the more intense peak in the (200) crystallographic plane. On the other hand, those films deposited with a F/Sn ratio = 0 (pure tin oxide) shows a preferred orientation in the (211) plane and other peaks in the (101), (110) and (301) planes. These results let us know that the grain orientation is highly affected by the fluorine content that makes possible the obtaining of highly oriented films.

Actually, the preferred orientation depends not only on the precursor solutions, as reported in tin oxide films prepared using CVD, but also on the film thickness [16]. **Figure 3** shows the films topography obtained using scanning electron microscopy (SEM).

The grain size values estimated from the XRD patterns using the Scherrer's law [17], which gives the coherence length perpendicularly to the substrate, are shown in **Figure 4**. The average grain size visualized by SEM, which corresponds to the grain size parallel to the substrate, is higher than the estimation from the analysis of the XRD spectra. The root mean square

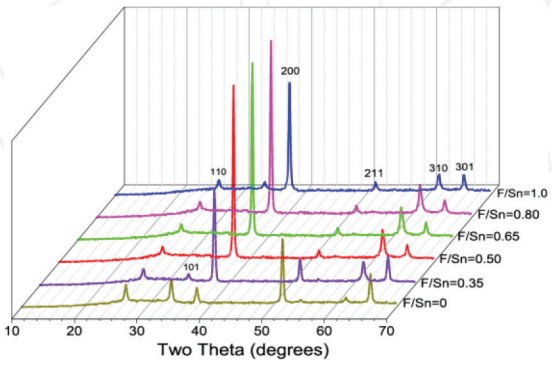

Figure 2. XRD spectra of FTO films with a thickness of around 500 nm and different F/Sn ratios in the precursor.

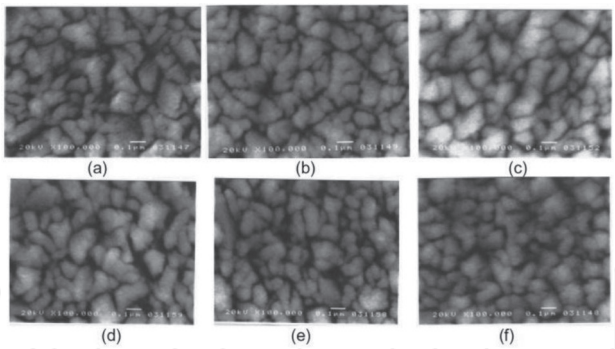

Figure 3. SEM images of the FTO films prepared using the solution with different F/Sn molar ratios. (a) F/Sn = 0; (b) F/Sn = 0.35; (c) F/Sn = 0.50; (d) F/Sn = 0.65; (e) F/Sn = 0.85; (f) F/Sn = 1.0.

(RMS) surface roughness of the FTO films for different F/Sn ratios is also shown in **Figure 4**. The highest grain size (~40 nm) and smallest RMS roughness (~8 nm) were observed for the films prepared using the precursor solution with the F/Sn ratio = 0.5. The films fabricated using the precursor solution with this fluorine concentration present a more arranged grain structure, whereas the increment of the roughness for films with a higher fluorine concentration can be connected with the etching by gaseous HF formed by the thermal decomposition of NH_4F during the growth process.

Figure 5 shows the dependence of the electrical resistivity (ρ), Hall mobility (μ), and carrier density (n) for the 500 nm thick FTO films on different F/Sn ratios. The films fabricated using the precursor with F/Sn ratio = 0.5 show the minimum resistivity, $\rho = 2.2 \times 10^{-4}$ Ω·cm (or Rs = 4.5 Ω^{-2}), as well as the higher carrier mobility and density, $\mu = 21.6$ cm^2/V s and $n = 1.7 \times 10^{21}$ cm^{-3}, respectively. Assuming an electron effective mass of 0.33 m_0 [18], the threshold carrier

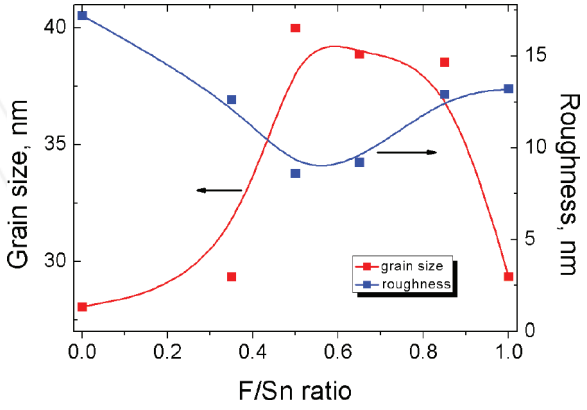

Figure 4. Mean value of the grain size for the (200) plane and the RMS surface roughness for the FTO films prepared using the solution with different F/Sn ratios.

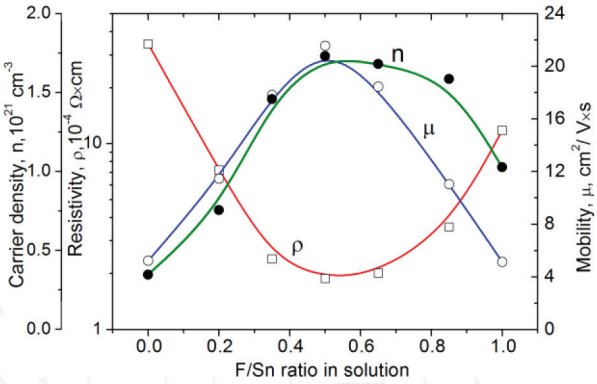

Figure 5. Resistivity (ρ), Hall mobility (μ), and carrier density (n) for the FTO films prepared using solutions with different F/Sn ratios.

density corresponding to strong degeneration in the conduction band for the FTO films is 3.6×10^{18} cm^{-3}. Electron concentration and Hall mobility increase for a higher fluorine content due to this doping effect and the improvement of the film structure. On the other hand, these parameters deteriorate when inside the film, and there is a formation of Sn-F dissipation neutral centers for carriers as well as due to a reduction in the oxygen vacancies for an increasing F/Sn ratio. In an early publication [19], we present a more detailed discussion of these results. A reduction in the mobility cannot be explained as due to the high carrier density, but as due to the electron scattering by ionized impurities and by neutral centers that are formed by the Sn-F bounds shown by XPS measurements. The mean free path of conduction electrons has the same dependence as the carrier density and shows a maximum of 5.3 nm for F/Sn = 0.5. Since the mean free path is considerably shorter than the grain size (30–40 nm), the resistivity of the films is determined by the ionized impurity scattering rather than by the grain boundary scattering.

Figure 6 shows the transmittance of the 500 nm thick FTO films deposited on Corning glass substrates using the precursor solutions with different F/Sn ratios. The transparency of the films exceeds 80% in the visible spectral range.

For highly degenerated FTO films, the value of the optical gap (**Figure 7**) is determined by a blue shift of the high-energy photon absorption edge due to the location of the Fermi level inside the conduction band. This effect is known as the Burstein-Moss shift. Hence, the lowest states in the conduction band are blocked, and the transitions of optically excited electrons take place only to energies above the Fermi level.

The films with F/Sn ratio = 0.5 that present an optical energy gap of 4.6 eV due to a high value of the Burstein-Moss shift; this is very useful for designing UV semiconductor photodetectors by increasing their conversion efficiency. Subsequently, we discussed the practical applications of this effect for designing an effective surface-barrier UV photodetectors with the FTO films as a transparent conducting active electrode.

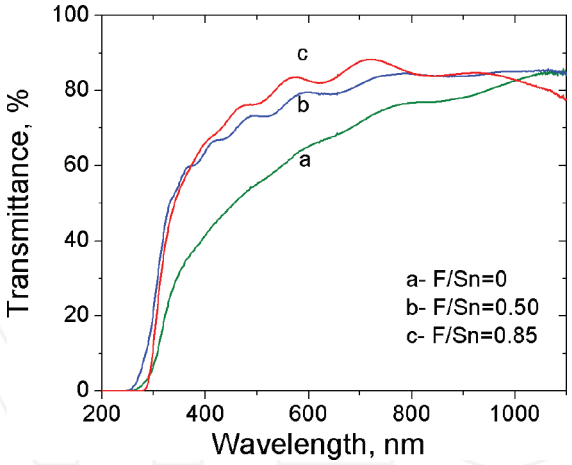

Figure 6. Transmittance of the 500 nm thick FTO films deposited using the precursor solutions with different F/Sn ratios on Corning glass substrates.

For quality estimation and comparative analysis of the TCO films fabricated by different methods and having different thicknesses, Haacke [20] proposed a revised figure of merit (FOM) defined by

$$\phi_H = \frac{T^{10}}{R_s} \tag{1}$$

where R_s and T represent the sheet resistance and transmittance, respectively.

A higher value of FOM indicates a higher performance of a film characterized simultaneously with low sheet resistance and high transparency. However, the FOM cannot be unlimitedly high. For commercial FTO films, the reported FOM is $17.4 \times 10^{-3}\ \Omega^{-1}$ [6], and the highest known Haacke FOM value for such films is $35.7 \times 10^{-3}\ \Omega^{-1}$ [7]. A different approach for the calculation

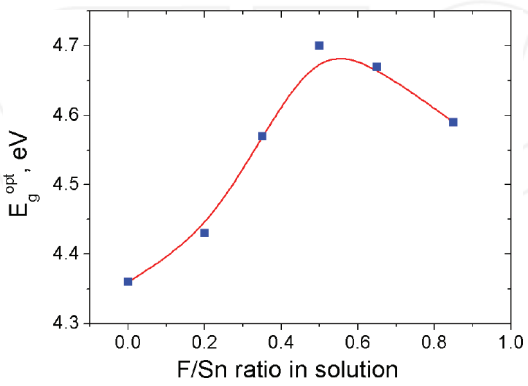

Figure 7. Value of the optical gap for FTO films fabricated from the solutions with different F/Sn ratios.

of the FOM was proposed by Gordon [8] to determine the FOM as the ratio of the electrical conductivity σ to the absorption coefficient α in the visible wavelength range.

$$\phi_G = \frac{\sigma}{\alpha} = \frac{1/R_s t}{\frac{-\ln(T+R)}{t}} = -[R_s \ln(T+R)]^{-1} \quad (2)$$

where t is the film thickness, R_s is the sheet resistance in ohms per square (Ω^{-2}), T is the total visible transmittance, and R is the total visible reflectance. From this point of view, a FOM = 3 Ω^{-1} is reported for CVD fluorine-doped tin oxide films with R_s = 8 Ω^{-2} and visible absorption coefficient α = 0.04 1/cm. Other authors [9] report higher values of FOM = 5.3 Ω^{-1} for FTO films fabricated using aerosol-assisted CVD. The commercial FOM standard for FTO films lies in the 1.5–1.6 Ω^{-1} range.

The best-known value of the FOM=7 Ω^{-1} is also reported by Gordon [10] for fluorine-doped zinc oxide films. The use of this method requires the measurement of the reflectance and the transmittance spectra, which is a disadvantage, however, has been adopted to establish the TCO films FOM for developing thin film solar cells modules.

In this work, we used both methods for the calculation of the FOM (ϕ), proposed by Haacke (ϕ_H) and by Gordon (ϕ_G). For using the Haacke method, the wavelength of the transmittance must be in the visible spectral range, though a specific wavelength is not determined. This leads to some uncertainty on the calculation of the FOM reported by different authors because of the strong dependence of the transmittance on the precise wavelength values. Furthermore, a strong interference effects on the films, as well as a significant difference in the maximum and minimum transmittance, strengthens this speculation.

The experimental reflectance and transmittance of the films must be integrated in order to calculate the Gordon FOM in the visible spectral range. We show in **Table 3** a comparison of the highest FOM reported from different authors with those obtained in this work using both methods.

Fabrication method	Sheet resistance, Ω^{-2}	Transmittance, %	f_H, 10^{-3} W^{-1} (Haacke)	f_G, W^{-1}, (Gordon)	Reference
CVD, commercial	7	80–82	15.4–19.6	…	[6]
Spray pyrolysis	5.1	85 (550 nm)	35.7	…	[7]
CVD	8	~84	…	3	[8]
Aerosol-assisted	3.9	82 (400–700 nm)	35.2	5.3	[9]
Spray pyrolysis	4.5	84 (400–700 nm)	38.8	5.75	This work

Table 3. The comparison of the highest FOM values reported by different authors.

4. Spray-deposited tin-doped indium oxide films

Tin-doped indium oxide (ITO) films are more widely used for different optoelectronic applications. Spray pyrolysis is the cheapest fabrication method allowing the obtaining of ITO films with high level of electric and optical parameters. Usually, the films are fabricated by spraying

solutions of $InCl_3 \cdot 4H_2O$ in ethanol. A small amount of tin chloride ($SnCl_4 \cdot 5H_2O$) is added as dopant. A detailed fabrication technique using such precursor has been described earlier [4]. **Table 4** shows the amount of the tin chloride in 25 ml 0.35 molar solution of $InCl_3 \cdot 4H_2O$ in ethanol to obtain different Sn/In ratios in the precursor solution.

The properties of the ITO films fabricated by spray pyrolysis on heated glass substrates depend strongly on the deposition parameters. Films fabricated in optimal conditions at a temperature of 480°C using the precursor solution with In/Sn ratio around 5% present the highest electric and optical parameters in comparison with films prepared by DC sputtering [20]. It was found that to obtain high-performance sputtered films, an additional annealing in an oxygen atmosphere is necessary [21]; this comparison is shown in **Table 5**.

Some works, for instance [22], were conducted for determining the dependence of the film parameters deposited by the spray pyrolysis method on the variation of the solvent in the spraying solution. It was found that organic solvents, such as ethanol and methanol, are more suitable in comparison with water for obtaining high-quality ITO films. A lower resistivity 2.5×10^{-4} Ω·cm was obtained using the methanol as solvent. The resistivity of the films fabricated using solutions in which water serves as solvent was in the range of 10^{-3} Ω·cm. However, the work function of the ITO films increases when an organic solvent mixed with water was used.

As a basic substance for preparation of the spraying solutions other indium compounds can be used, such as Indium (III) acetate, $In(OOCCH_3)_3$ dissolved in methanol. In this case, tin chloride ($SnCl_4 \cdot 5H_2O$) can be used for doping. Subsequently, the properties of the ITO films fabricated on glass substrates heated to 460°C using such precursor solutions are reported. Different Sn/In ratios in the precursors were used for the determination of the optimum tin content in the spraying solution. A ratio of Sn/In = 6%% corresponds to an optimal doping concentration for obtaining films with the minimum resistivity (**Figure 8**). For all the Sn/In ratios used in the solution, the films fabricated were nanocrystalline with a (400) columnar orientation of grains (inset in **Figure 8**).

The size of grains is around 150–180 nm. The sheet resistance of the 400 nm thick ITO films fabricated from the precursor solution with an optimal Sn/In ratio was $R_s = 5.5\ \Omega^{-2}$. The electron density and the Hall mobility were around 10^{21} cm^{-3} and 28.5 $cm^2/V \times s$, respectively. Transmittance spectrum of such films without influence of the substrate is shown in **Figure 9**.

The figure of merit FOM = $57 \times 10^{-3}\ \Omega^{-1}$ was determined from the experimental values of R_s and integral value of the transmittance $T = 0.89$ in visible and near infra-red spectral range.

Sn/In ratio in solution	0	0.02	0.03	0.05	0.07	0.09	0.11
$SnCl_4 \cdot 5H_2O$, mg	0	61.2	92.0	153.3	214.7	276.0	337.4

Table 4. Amount of $SnCl_4 \cdot 5H_2O$ for obtaining different Sn/In ratios in the $InCl_3 \cdot 4H_2O$ ethanol solution.

http://dx.doi.org/10.5772/67431

Parameters	Sputtered and annealed ITO film	Spray-deposited ITO film
Annealing temperature, °C	300	–
Ratio Sn/In in solution, %	–	5
Substrate roughness (nm)	2.7	2.7
Ratio XRD peaks (222/400)	1.23	0.032
Grain size (nm)	45.0	165
ITO roughness (nm)	0.43	30
Specific resistance (10^{-4} Ω·cm)	2.8	2.3
Carrier concentration (10^{20} cm^{-3})	11.8	10
Mobility ($cm^2V^{-1}s^{-1}$)	22.0	28
Integral transparency	0.83	0.88
FOM (10^{-3} Ω^{-1})	12.5	23

Table 5. The comparison properties of sputtered and sprayed ITO films [20, 21].

Table 6 shows a comparison of this FOM value with that reported in the literature for ITO films with different thickness fabricated by different methods.

According to the high FOM obtained for ITO films deposited from a spraying solution based on indium acetate in ethanol, it is possible to conclude that this method allows for the fabrication of high-quality tin-doped indium oxide films for a number of optoelectronics applications.

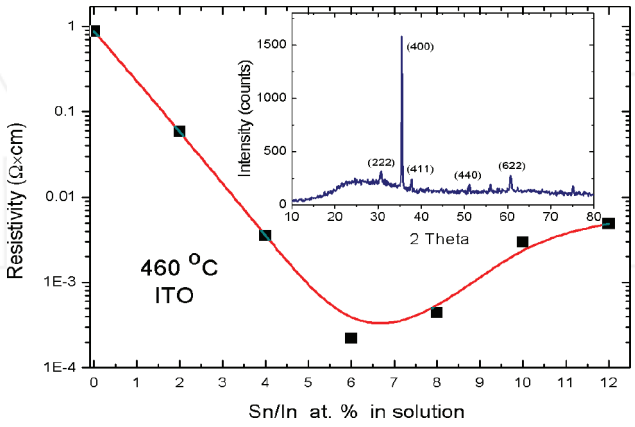

Figure 8. Resistivity of the ITO films fabricated using an indium acetate solution with different Sn/In ratios. The inset shows the XRD spectra of the ITO films with a 6 at.% of Sn/In ratio.

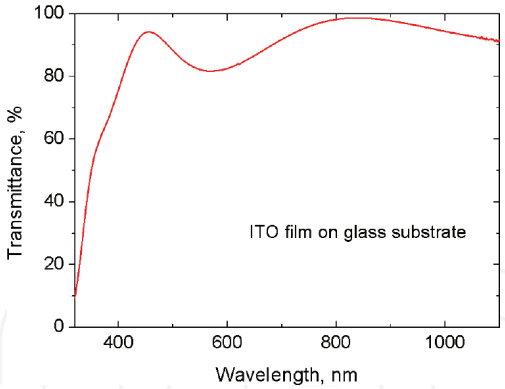

Figure 9. Transmittance of the ITO films fabricated using an indium acetate solution with a Sn/In= 6 at.% ratio.

Deposition method	R_s, Ω^{-2}	Transmittance, %	FOM, 10^{-3} Ω^{-1}	Reference
Spray pyrolysis	26	90	13.4	[23]
Spray pyrolysis	9.3	85	21	[24]
Reactive evaporation	25	98	32.7	[25]
Dip coating	7.1	78	11.7	[26]
Sputtering DC	22	92	19.7	[27]
Spin coating	30	90.2	11.9	[28]
This work	5.5	89	57	This work

Table 6. Comparison of the FOM obtained in this work using the spray pyrolysis method with that reported in literature for ITO films fabricated by other methods.

5. Spray-deposited aluminum and indium-doped zinc oxide films

The undoped zinc oxide (ZnO) thin films, with an energy band gap of 3.3 eV, present a high electrical resistivity and are used for several applications. For example, they have piezoelectric properties and their highly oriented texture may be of interest for high-frequency electroacoustic transductors. When ZnO films are doped with indium [29, 30] or aluminum [31], the films present a high conductivity. Due to the high conductivity and transparency in visible region of the spectrum, the doped zinc oxide films are of great interest as transparent conductors in optoelectronic displays, photovoltaic structures, thermal reflecting layers, and also when used as a sensitive element in gas sensors. The spray pyrolysis method is very suitable for the fabrication of high transparent and low conductive ZnO films [32–36]. Precursors for the spraying alcoholic solution containing zinc ($ZnCl_2$, $Zn(NO)_2$, Zn acetate, etc.) are cheaper than

http://dx.doi.org/10.5772/67431

those containing indium. The precursors for doping may be $InCl_3$ and $AlCl_3$ [37, 38]. However, the fabrication of In- or Al-doped ZnO films with low resistivity by spray pyrolysis without a postannealing processing does not lead to the expected results [39].

In this work, undoped and In- and Al-doped ZnO films were grown on borosilicate glass substrates by spray pyrolysis at 500°C. A 0.3 molar solution was made by dissolving zinc acetate in a 3:1 mixture of methanol and water. For doping purposes, $InCl_3$ or $AlCl_3$ was added in the spraying solution. The atomic ratio of In/Zn or Al/Zn in the solution was kept in the range 1–5%. After the deposition, some films were annealed at 300°C during 30 min in high vacuum or in argon atmosphere.

The X-ray diffraction spectra of the undoped and doped annealed ZnO films show a ZnO-single phase with an hexagonal wurtzite structure [40] as shown in **Figure 10**.

All the films are nano-crystalline with grain sizes between 40 and 60 nm, as determined by the Debye-Scherrer method [41].

Introduction of indium in ZnO matrix changes the preferred grain orientation from (101) for undoped ZnO films to (002) for In-doped ZnO films. Annealing in argon atmosphere leads to a more pronounced enhancement of the grain sizes for Al-doped ZnO films. The SEM images of the grown films are shown in **Figure 11**.

From **Figure 11**, it is clear that the In-doped films are smoother than the undoped and Al-doped ZnO films.

The variation of resistivity of the films as a function of doping and thermal treatment is shown in **Figure 12** [39]. It was found experimentally that the lowest resistivity is presented by the films with a ratio of Al/Zn or In/Zn around 3%. Annealing reduces the resistivity when this is conducted in an argon atmosphere. This fact can be explained as due to the desorption of chemisorbed oxygen at the grain boundaries [42], leading to an annihilation of the oxygen acceptor states at the grain boundaries, which act as traps for electrons.

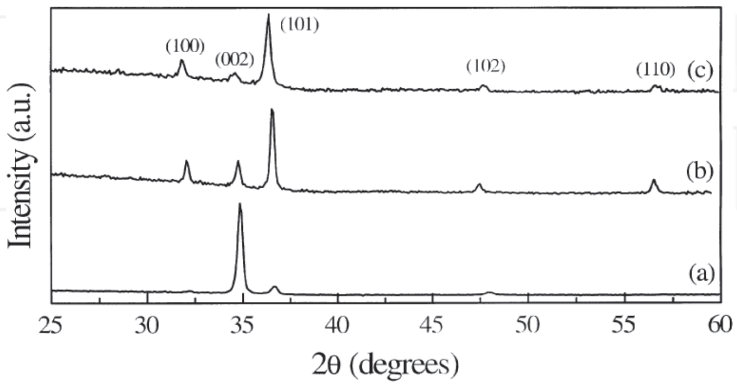

Figure 10. X-ray diffraction spectra for undoped ZnO (a), Al-doped ZnO (b), and In-doped ZnO (c) films.

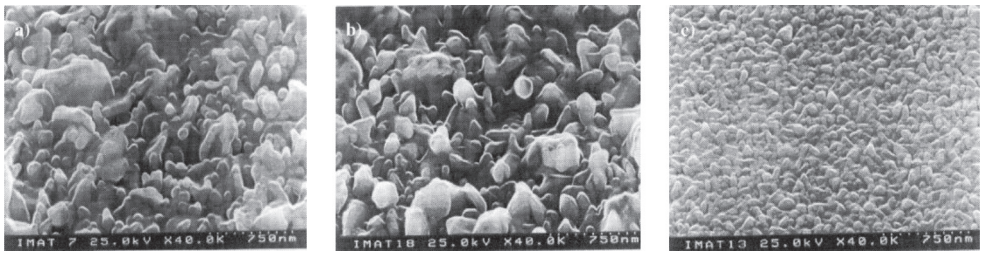

Figure 11. SEM images of undoped ZnO (a), Al-doped ZnO (b), and In-doped ZnO (c) films.

The Hall effect data show that the films are n-type with a mobility ranging from 1.8 to 13 $cm^2V^{-1}s^{-1}$ when the films were annealed in argon atmosphere. The highest value of mobility is observed for the In-doped ZnO films fabricated using a solution with an In/Zn ratio of about 3%. The worse structural and electrical characteristics of Al-doped ZnO films could be explained as due to an interstitial insertion of Al atoms in the ZnO lattice leading to a distortion of the crystalline lattice and disorder in the grains orientation.

The transmittance spectra of the films in the visible and near infra-red spectral range are above 80%. A reduction in the transmittance could be explained by the light scattering (haze), and this is directly connected with the films morphology. Light scattering can be characterized by the haze factor defined as the ratio between the diffuse transmittance measured in a photometric sphere and the total transmittance (diffuse + specular). The haze factor depends on the wavelength and serves as an indicator for the light-scattering capability of diffusing

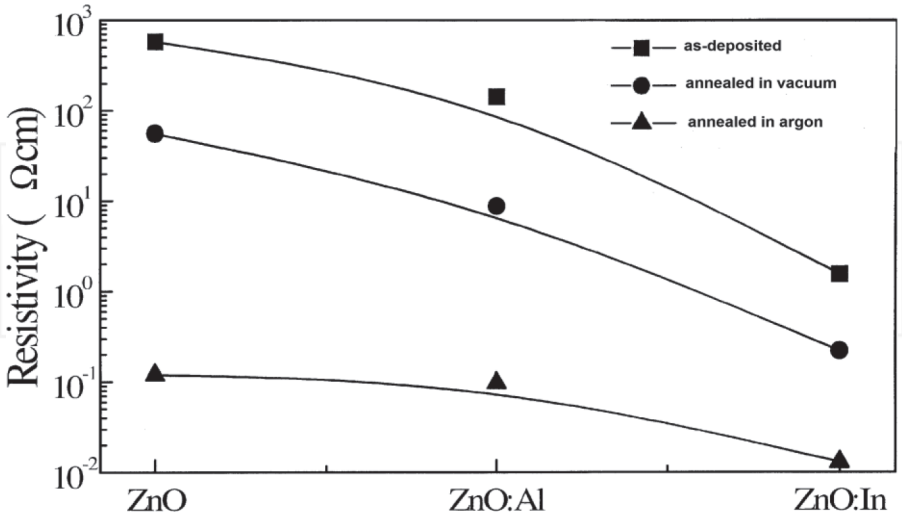

Figure 12. Resistivity as a function of the annealing atmosphere for undoped, Al-doped, and In-doped ZnO films.

http://dx.doi.org/10.5772/67431

transparent conducting films used in thin film solar cell applications. Textured surfaces of the films lead to an enhancement on the light collected into thin film photovoltaic structures. Al-doped ZnO films a higher haze factor, 30%, in comparison with undoped ZnO films (haze factor = 19%) and In-doped ZnO films (haze factor = 0.85 for In/Zn = 3 at.%). It is directly connected with the films morphology shown in **Figure 11**, which indicates that Al disturbs strongly the film structure.

Figure 13 shows the transmittance spectra of undoped and In-doped ZnO films. The In/Zn ratios are shown in the inset of the figure. Values of figure of merit (FOM) for the undoped and doped ZnO films differ a lot from those reported above for FTO and ITO films. As deposited, the ZnO films present low FOM values in the range of $2.5 \times 10^{-7}\ \Omega^{-1}$ for undoped films to $2.8 \times 10^{-5}\ \Omega^{-1}$ obtained for In-doped films.

The highest FOM = $3.7 \times 10^{-3}\ \Omega^{-1}$, after annealing in argon, is presented by the In-doped ZnO films. However, it is one order of magnitude below the best FOM for FTO and ITO films. Undoubtedly, spray-deposited doped ZnO films is of great interest for optoelectronic applications, but for fabrication such films with high FOM values, a further investigation is necessary.

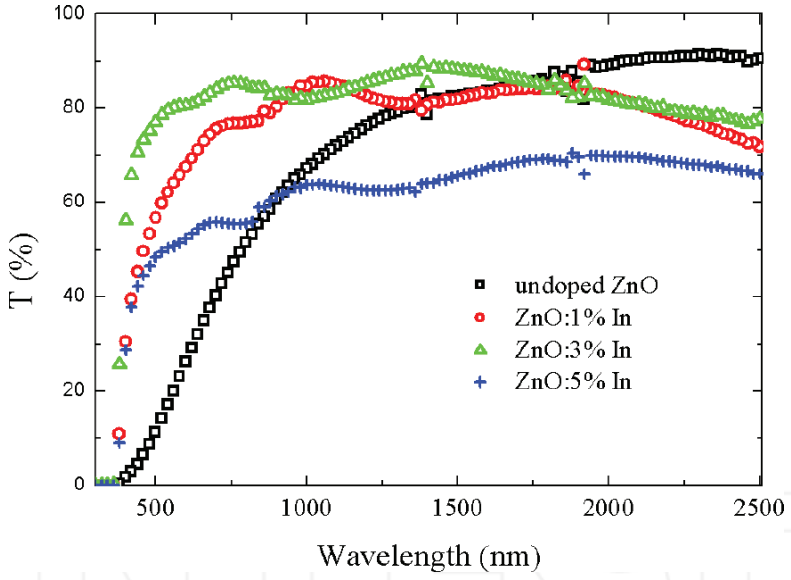

Figure 13. The transmittance spectra of undoped and In-doped ZnO films.

6. Spray-deposited fluorine-doped titanium dioxide films

In several applications such as in sensors, pigments, protective coatings, dye-sensitized solar cells, and photocatalysis [43] titanium oxide (TiO_2) has been found to be attractive. Due to

its nontoxicity, high efficiency with a low cost, and biological and chemical stability, TiO_2 is probably the most studied photocatalyst. Titanium dioxide films are very attractive to optoelectronic applications, such as electrochemical solar cells, antireflection coatings, and protective layers, to prevent plasma reduction of transparent conductive oxides in thin film solar cells. Because of its simplicity, spray pyrolysis is an attractive method for the fabrication of these films [44–46].

We demonstrate the influence of fluorine on the structural and optical properties of titanium dioxide films, prepared by spray pyrolysis on glass substrates at 470°C, using $Ti(OC_3H_7)$ alcoholic solutions with an addition of fluorine in the form of NH_4F, over a large range of fluorine to titanium atomic ratio in the solution. The characterization was performed using X-ray diffraction analysis and measurements of transparency. Without NH_4F in the starting solution, the formation of titanium dioxide layers was not possible . A high amount of ammonium fluoride (F/Ti ratio in solution about of 8.5 at.%) resulted in the formation of a white hygroscopic powder, probably of polymeric nature. The formation of transparent (above 85%) and nano-crystalline TiO_2 films depends strongly on the F/Ti ratio in the spaying solution. Films prepared using a solution with F/Ti <1.5 at.% present an amorphous structure and rough surface, with an integral haze factor near 20%. Films fabricated using a solution with F/Ti ratio near 1.5–1.6 at.%, present a nanocrystalline structure, not usually observed, *brookite* structure, an orthorhombic crystalline structure with a unit cell described by the space group Pbca [47, 48], and their XRD patterns consist only in one (121) sharp peak (**Figure 14**). Such films have a smoother surface (optical haze factor <10%).

Edge absorption measurements show that the absorption coefficient above the threshold of fundamental absorption follows the $(E–E_g)^{1/2}$ energy dependence characteristic of direct allowed transitions (determined value of energy gap E_g is 3.72 eV), in contrast to the indirect

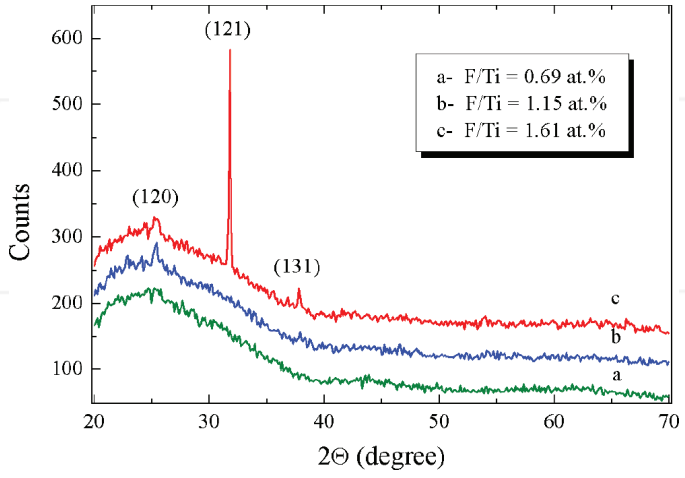

Figure 14. XRD spectra of fluorine-doped TiO2 films fabricated by spray pyrolysis.

transitions in TiO_2 films either with rutile or anatase crystalline structure (E_g = 3.03 eV and 3.2 eV, respectively). The synthesis of fluorine-doped TiO_2 powder was reported by using the spraying of an aqueous solution of H_2TiF_6 with F/Ti ratio from 2.76% to 9.40% at 1173 K [43]. Additional works reporting fluorine-doped titanium dioxide was not found. Undoubtedly, further investigation in this field must be of interest. Pure brookite has demonstrated to be an interesting candidate in photocatalytic applications, and the number of papers on the preparation and photocatalytic activity of the TiO_2 with brookite structure has increased exponentially by 100 times in the past 10 years [48].

7. Application of TCO films in optoelectronic devices

The spray pyrolysis method for the fabrication of high-quality TCO films has been successfully applied to the development of simple but enough effective optoelectronic devices. Readers have found a detailed description of useful effective photoelectronic devices based on surface barrier heterojunctions in our published works [49–58].

The physics of surface-barrier (SB) devices is based on the well-known Schottky barrier that is a potential energy barrier for carriers formed at a metal-semiconductor (M-S) junction [59]. In the design of SB devices, the main function of the barrier is to separate carriers photogenerated inside the semiconductor substrate. Such optoelectronic devices are very simple structures because they are unnecessary for the formation of a p-n junction by high-temperature processes. SB optical detectors operate without optical losses in the highly doped p-layer and also present a very high speed of response for a modulated optical signal. The SB structure is very useful for the fabrication of optoelectronic semiconductor devices in which a p-n junction cannot be created due to doping troubles. At the same time, in order to use M-S structures as radiation detectors, the metal electrode must be extremely thin (<15 nm) to prevent the losses of the radiation absorption and also must be chemically resistant to prevent device degradation in time (thinner metallization leads to devices susceptible to degradation). Among the several metals available, only some of them such as Au, Pt, Ni are suitable for this applications. Moreover, the high reflectivity of these metallic layers demands the use of antireflection coatings. The electrical properties of SB photodetectors based on M-S structures can be enhanced by the introduction of a very thin (<3 nm) insulating layer between the metallic film and the semiconductor (M-I-S structures). The presence of this insulator layer reduces the number of localized states at the semiconductor interface and hence serves to reduce the interface carrier recombination. Its presence can also reduce significantly the thermo ionic emission current because of an increase in the potential barrier for majority carriers [60]. In this case, the thickness of the insulating layer must not reduce the transport of minority carriers from the semiconductor to the metal.

In order to obtain the best photoelectrical properties of SB radiation detectors based on M-S and M-I-S structures, the metallic opaque layer can be changed by a thin film based on some transparent conducing oxide (TCO), such as tin-doped indium oxide (ITO) or fluorine-doped

tin oxide (FTO), which are widely used for optoelectronic applications. In such structures, the TCO films operate as an active metal-like transparent conducting electrode. Thickness tuning of the TCO films allows for its use as an effective antireflection coating for reducing the radiation losses. The spray pyrolysis is the simplest method used for the deposition of such films with high electrical and optical parameters.

Detailed characteristics of optoelectronic devices will be published soon. Here, we present only some general characteristics to demonstrate the usefulness of the TCO films. **Figure 15** shows the spectral response of high-speed SB photodiodes for ultra-violet, visible, and near infra-red spectral range fabricated by the deposition of the ITO or FTO film on the surface of some epitaxial semiconductors structures, GaP, AlGaAs compounds, and Si. Density of a dark current does not exceed a value in the 10^{-9}–10^{-6} A/cm^2 range.

Figure 16 shows the current-voltage characteristic (a) and output power (b) of a solar cell under AM1 solar illumination fabricated on monocrystalline silicon by deposition of a high-quality ITO film on a chemically treated silicon surface [59, 60]. The efficiency of such low cost in the fabrication of solar cells is around 13%.

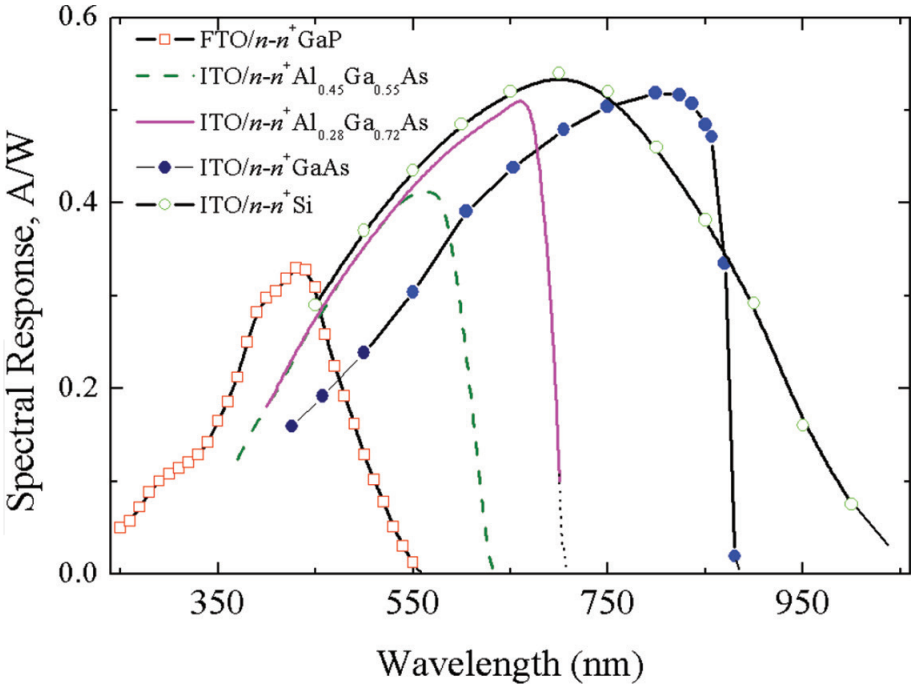

Figure 15. The spectral response of the surface-barrier photodiodes fabricated by spray deposition of the ITO and FTO films on the surface of the semiconductor epitaxial structures.

http://dx.doi.org/10.5772/67431

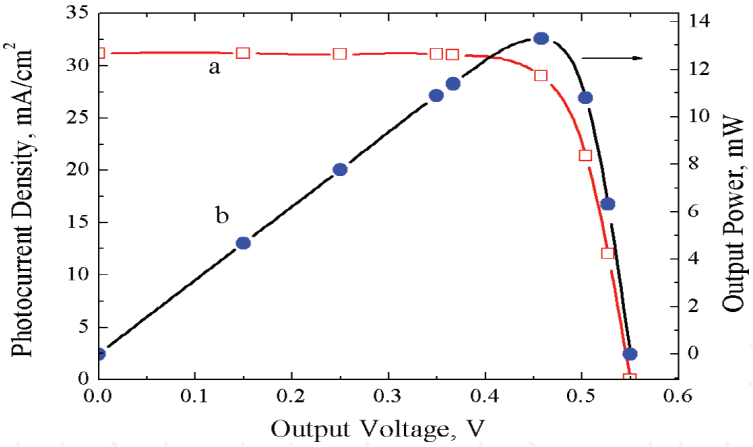

Figure 16. Current-voltage characteristic of a solar cell under AM1 solar illumination fabricated on monocrystalline silicon by deposition of high-quality ITO film on a chemically treated silicon surface.

8. Conclusion

We report some basic knowledge about the spray pyrolysis method for the fabrication of high-quality transparent conducting oxide films used for optoelectronic applications. This is a low cost though an efficient method that has been used for the deposition of fluorine-doped tin oxide, tin-doped indium oxide, indium- or aluminum-doped zinc oxide, and fluorine-doped titanium dioxide films and other semiconductor and dielectric thin films. The high-level electrical and optical parameters of these films prove that this method is very suitable for the fabrication of different optoelectronic devices.

Author details

Oleksandr Malik[1,*], Francisco Javier De La Hidalga-Wade[1] and Raquel Ramírez Amador[2]

*Address all correspondence to: amalik@inaoep.mx

1 National Institute for Astrophysics, Optics and Electronics, INAOE, Puebla, Mexico

2 Technical University of Huejotzingo, Puebla, Mexico

References

[1] Handbook of transparent conductors. D. S. Ginley, H. Hosono, and D. C. Paine, Eds. 2010. Springer, New York.

[2] R. R. Chamberlin, J. S. Skarman. Chemical spray deposition process for inorganic films-. J. Electrochem. Soc. 1966; 113(1): 86-89; doi:10.1149/1.2423871

[3] P. S. Patil. Versatility of chemical spray pyrolysis technique. Mater. Chem. Phys. 1999; 59: 185-198.

[4] O. Malik, F. J. De la Hidalga-W. Physical and technological aspects of solar cells based on metal oxide-silicon contacts with induced surface inversion layer. In: Application of Solar Energy, R. Rugescu Ed. 2013. Intech, Croatia. ISBN 978-953-51-0969-3

[5] J. B. Mooney, S. B. Radding. Spray pyrolysis processing. Annu. Rev. Mater. Sci. 1982; 12: 81-101.

[6] J. C. Viguié, J. Spitz. Chemical vapor deposition at low temperatures. J. Electrochem. Soc. 1975; 122(4): 585-588.

[7] G. J. Exarhos, X-D. Zhou. Discovery-based design of transparent conducting oxide films. Thin Solid Films. 2007; 515: 7025-7032.

[8] Y. Sawada, C. Kobayashi, S. Seki, and H. Funakubo. Highly conducting indium-tin-oxide transparent films fabricated by spray CVD using ethanol solution of indium (III) chloride and tin (IV) chloride. Thin Solid Films. 2002; 409: 46-50.

[9] T. Fukano, T. Motohiro. Low-temperature growth of highly crystallized transparent conductive fluorine-doped tin oxide films by intermittent spray pyrolysis deposition. Sol. Energ. Mater. 2004; 82: 567-575.

[10] B. Benhaoua, S. Abbas, A. Rahal, A. Benhaoua, and M. S. Aida. Effect of film thickness on the structural, optical and electrical properties of SnO_2:F thin films prepared by spray ultrasonic for solar cells applications. Superlattices Microstruct. 2015; 83: 78-88.

[11] L. Filipovic, S. Selberherr, G. C. Mutinati, E. Brunet, S. Steinhauer, A. Kock, J. Teva, J. Kraft, J. Siegert, and F. Schrank. Modeling spray pyrolysis deposition. In: Proceedings of the World Congress on Engineering. 2013; Vol II. London, UK. ISBN: 978-988-19252-8-2.

[12] A. Malik, V. Baranyuk, and V. Manasson. Solar cells based on the SnO_2-SiO_2-Si heterojunction. Appl. Sol. Energ. 1979; 2: 83-84. ISSN: 0003-701x.

[13] A. Malik, V. Baranyuk, and V. Manasson. Improved model of solar cells based on In_2O_3/SnO_2-SiO_x-nSi structures. Appl. Sol. Energ. 1980; 1: 1-2.

[14] O. Malik, F. J. De la Hidalga-Wade, and R. R. Amador. Fluorine-doped tin oxide films with a high figure of merit fabricated by spray pyrolysis. J. Mater. Res. 2015; 30(13): 2040-2045.

[15] Joint Committee on Power Diffraction Standards (JCPDS). International Centre for Diffraction Data. 1997; Card No. 41-1445.

[16] K. H. Kim and J. S. Chun: X-ray studies of SnO_2 prepared by chemical vapor deposition. Thin Solid Films. 1986; 141: 287-292.

[17] J. W. Kim, H. S. Kang and S. Y. Lee. Effect of deposition rate on the property of ZnO thin films deposited by pulsed laser deposition. J. Electr. Eng. Technol. 2006; 1; 98-105.

[18] E. Shanthi, A. Banerjee, and K. L. Chopra: Dopant effects in sprayed tin oxide films. Thin Solid Films. 1982; 88: 93 -.

[19] A. I. Martínez, L. Huerta, J. M. O-Rueda de León, D. Acosta, O. Malik, and M. Aguilar: Physicochemical characteristics of fluorine doped tin oxide films. J. Phys. D: Appl. Phys. 2006; 39: 5091-.

[20] O. Malik, F. J. De la Hidalga-W. Spray deposited thin films of tin-doped indium oxide for optoelectronic applications. Adv. Mat. Res. 2013; 677: 173-178.

[21] O. Malik, F. J. De la Hidalga-W. Comparison of tin-doped indium oxide films fabricated by spray pyrolysis and magnetron sputtering. Cryst. Res. Technol. 2015; 50: 516-520.

[22] T. Ishido, H. Kouno, H. Kobayashi, and Y. Nakato. Dependence of photovoltages of spray-deposited indium tin oxide/silicon oxide/silicon junction solar cells on spray solvents. J. Electrochem. Soc. 1994; 141(5): 1357-1361.

[23] V. Vasu, and A. Subrahmanyam. Reaction kinetics of the formation of indium tin oxide films grown by spray pyrolysis. Thin solid Films. 1990; 193/194: 696-703.

[24] J. C. Manifacier, J. P. Fillard, and J. M. Bind. Deposition of In_2O_3-SnO_2 layers on glass substrates using a spraying method. Thin Solid Films. 1981; 77: 67-80.

[25] P. Nath, R. F Bunshah. Preparation of In_2O_3 and tin-doped In_2O_3 films by a novel activated reactive evaporation technique. Thin Solid Films. 1980; 69: 63-68.

[26] S. Seki, Y. Sawada, M. Ogawa, M. Yamamoto, Y. Kagota, A. Shida, and M. Ide. Highly conducting indium tin-oxide transparent films prepared by dip-coating with an indium carboxylate salt. Surf. Coat. Technol. 2003; 169:525–527.

[27] U. Betz, M. K. Olsson, J. Marthy, M. F. Escola, F. Atamny, Thin films engineering of indium tin oxide: large area flat panel displays application. Surf. Coat. Technol. 2006; 200: 5751–5759.

[28] Z. Chen, W. Li, Ran Li, Y. Zhang, G. Xu, and H. Cheng. Fabrication of highly transparent and conductive indium tin oxide thin films with a high figure of merit via solution processing. Langmuir. 2013; 29: 13836–13842.

[29] S. N. Qiu, C. X. Qiu, and I. Shih. Air heat treatment of In-doped ZnO thin films. Sol. Energ. Mater. 1987; 15: 261-267.

[30] Sh. El Yamny, M. Abdel Rafea. Preparation and characterization of ZnO: in transparent conductor by low cost dip coating technique. J. Mod. Phys. 2012; 3: 1060-1069.

[31] C. Lennon, R. Kodama, Y. Chang, S. Sivanathan, and M. Deshpande. Al- and Al:In-doped ZnO thin films deposited by RF magnetron sputtering for spacecraft charge mitigation. J. Electron. Mater. 2008; 37(9): 1324-1328.

[32] J. Aranivich, A. Ortiz, and R. H. Bube. Optical and electrical properties of ZnO films prepared by spray pyrolysis for solar cell applications. J. Vac. Sci. Technol. 1979; 16: 994-1001.

[33] M. Krunks, E. Mellikov. Zinc oxide thin films by the spray pyrolysis method. Thin Solid Films. 1995; 270: 33-36.

[34] A. Ashour, M. A. Kaid, N. Z. El-Sayed. and A. A. Ibrahim. Physical properties of ZnO thin films deposited by spray pyrolysis technique. Appl. Surf. Sci. 2006; 252: 7844-7848.

[35] N. Lehraki, M. S. Aida, S. Abed, N. Attaf, A. Attaf, and M. Poulain. ZnO thin films deposition by spray pyrolysis: influence of precursor solution properties. Curr. Appl. Phys. 2012; 12: 1283-1287.

[36] A. Goyal, S. Kachhwaha. ZnO thin films preparation by spray pyrolysis and electrical characterization. Mater. Lett. 2012; 68: 354-356.

[37] K. Krunks, O. Bijakina, V. Mikli, T. Varema, and E. Mellikov. Zinc oxide thin films by spray pyrolysis method. Phys. Scr. 1999; T79: 209-212.

[38] M. A. Kaid, A. Ashour. Preparation of ZnO-doped Al films by spray pyrolysis technique. Appl. Surf. Sci. 2007; 253: 3029-3033.

[39] P. Nunes, A. Malik, B. Fernandes, E. Fortunato, P. Vilarinho, and R. Martins. Influence of the doping and annealing atmosphere on zinc oxide thin films deposited by spray pyrolysis. Vacuum. 1999; 52: 45-49.

[40] A. Cimino, G. Mazzone, P. Ports. Lattice parameter study of defective zinc oxide. Zinc excess and distortions in pure ZnO. Z. fuer Phys. Chem. (Muenchen, Germany). 1964; 41(3/4): 154-172. ISSN: 0044-3336.

[41] J. W. Kim, H. S. Kang, and S. Y. Lee. Effect of deposition rate on the property of ZnO thin films deposited by pulsed laser deposition. J. Electrical Eng. Technol. 2006; 1(1): 98-100.

[42] S. Major, A. Banerjee, K. L. Chopra. Annealing studies of undoped and indium-doped films of zinc oxide. Thin Solid Films. 1984; 122(1): 31-43.

[43] D. Li, H. Haneda, S. Hishita, N. Ohashi, and N. K. Labhsetwar. Fluorine-doped TiO_2 powders prepared by spray pyrolysis and their improved photocatalytic activity for decomposition of gas-phase acetaldehyde. J. Fluor. Chem. 2005; 126: 69-77.

[44] I. Oja, A. Mere, M. Krunks, C-H. Solterbeck, and M. Es-Souni. Properties of TiO_2 films prepared by the spray pyrolysis method. Sol. State Phenom. 2004; 99/100: 259-264.

[45] L. Andronic, S. Manolache, and A. Duta. TiO_2 thin films prepared by spray pyrolysis deposition (SPD) and their photocatalytic activities. J. Optoelectron. Adv. Mater. 2007; 9(5): 1403-1406.

[46] N. C. Raut, T. Mathews, S. T. Sundari, T. N. Sairam, S. Dash, and A. K. Tyagi. Structural and morphological characterization of TiO_2 thin films synthesized by spray pyrolysis technique. J. Nanosci. Nanotechnol. 2009; 9(9): 5298-5302.

[47] L. Pauling, J. H. Sturdivant. The crystal structure of brookite. Z. Kristall. 1928; 68: 239-256.

[48] I. N. Kuznetsova, V. Blaskov, I. Stambolova, L. Znaidi, and A. Kanaev, TiO2 pure phase brookite with preferred orientation, synthesized as a spin-coated film. Mater. Lett. 2005; 59: 3820-3823.

[49] A. Malik, A. Seco, E. Fortunata, and R. Martins. New UV-enhanced solar blind optical sensors based on monocrystalline zinc sulphide. Sens. Actuators A. 1998; 67: 68-71.

[50] A. I. Malik, G. G. Grushka. Optoelectronic properties of metal oxide-gallium phosphide heterojunctions. Sov. Phys. Semicond. 1991; 25(10): 1017-1020. ISSN 0038-5700.

[51] A. Malik, A. Seco, E. Fortunato, R. Martins, B. Shabashkevich, and S. Piroszenko. A new high ultraviolet sensitivity FTO-GaP Schottky photodiode fabricated by spray pyrolysis. Semicond. Sci. Technol. 1998; 13: 102-107.

[52] Yu. Vygranenko, A. Malik, M. Fernandes, R. Schwarz, and M. Vieira. UV-visible ITO/GaP photodiodes: characterization and modeling. Phys. Stat. Sol. A. 2001; 185(1): 137-144.

[53] O. Malik, F. J. De la Hidalga-Wade, C. Zuniga-Islas, and J. Abundus Patiño. UV-sensitive optical sensors based on ITO-gallium phosphide heterojunctions. Phys. Stat. Sol. C. 2010; 7(3-4): 1176-1179.

[54] A. Malik, M. Vieira, and M. Fernandes. Surface-barrier Si-based photodetectors fabricated by spray pyrolysis technique. Philos. Mag. B. 2000; 80(4): 781-790.

[55] A. I. Malik, G. G. Grushka. Self-calibrated radiometric IR photodiode based on the defect semiconductor $Hg_3In_2Te_6$ for the spectral range 0.85− 1.5 μm. Soviet. Tech. Phys. 1990; 35: 1227-1231.

[56] A. I. Malik, M. Vieira, M. Fernandes, F. Macarico, and Z. Grushka. Near-infrared photodetectors based on HgInTe-semiconductor compound. Proceedings of SPIE 3629, Photodetectors: Materials and Devices IV. 1999: 433-442.

[57] O. Malik, F. J. De la Hidalga-W, C. Zúñiga-I, and G. Ruíz-T. Efficient ITO-Si solar cells and power modules fabricated with a low temperature technology: results and perspectives. J. Non Cryst. Solids. 2008; 354: 2472-2477.

[58] O. Malik, F. J. De la Hidalga-W. Physical and technological aspects of solar cells based on metal oxide-silicon contacts with induced surface inversion layer. In: Application of Solar Energy, R. Rugescu Ed. 2013. Intech, Croatia. ISBN 978-953-51-0969-3.

[59] R. T. Tung. The physics and chemistry of the Schottky barrier height. Appl. Phys. Rev. 2014; 1: 1-55.

[60] S. J. Fonash. Solar cell device physics. Academic Press. NY 1981: 331 p. ISBN 0-12-261980-3.

INTECH